

IMPROVEMENT OF TRANSIENT RESPONSE OF A DC GRID-BASED WIND POWER GENERATION SYSTEM IN A MICROGRID

P.Devika¹ | M. Rama Subbamma²

¹(M.Tech Scholar, Dept of EEE, Global College of Engineering & Technology, Kadapa, A.P, India)

²(Professor, Dept of EEE, Global College of Engineering & Technology, Kadapa, A.P, India)

Abstract—This paper presents the design of a dc grid-based wind power generation system in a poultry farm. The proposed system allows flexible operation of multiple parallel-connected wind generators by eliminating the need for voltage and frequency synchronization. A model predictive control algorithm that offers better transient response with respect to the changes in the operating conditions is proposed for the control of the inverters. The design concept is verified through various test scenarios to demonstrate the operational capability of the proposed micro grid when it operates connected to and islanded from the distribution grid, and the results obtained are discussed.

Keywords— Wind Power Generation; DC Grid; Energy Management; Model Predictive Control

1. INTRODUCTION

The Singapore government is effectively advancing this new concept of gathering wind vitality from electric ventilation fans in poultry ranches which has been executed in numerous nations around the globe. The significant distinction between the situation in poultry ranches and normal wind ranches is in the wind speed changeability. The inconstancy of twist speed in twist farms directly relies on upon the ecological and climate conditions while the twist speed in poultry ranches is for the most part steady as it is generated by consistent speed ventilation fans. In this way, the generation intermittency issues that influence the unwavering quality of electricity supply and power adjust are not pervasive in poultry cultivate wind energy systems. In late years, the exploration consideration on dc lattices has been resurging because of innovative progressions in control electronics and vitality stockpiling gadgets, and increment in the assortment of dc loads and the infiltration of dc Distributed Energy Resources(DERs), for example, sun based photovoltaic and fuel cells. Many look into deals with dc microgrids have been directed to encourage the coordination of different DERs and vitality stockpiling frameworks. In a dc microgrid base wind farm architecture in which each wind energy conversion unit consisting of a matrix converter, a high frequency transformer and a single-phase ac/dc converter is planned. However, the projected architecture increases the system difficulty as three stages of conversion are required. In a dc microgrid based wind farm architecture in which the WTs are clustered into groups of four with each group connected to a converter is proposed. However, with the proposed architecture, the failure of one converter will result in all four WTs of the same group to be out of service. The research works conducted in are focused on the development of different distributed control strategies to coordinate the operation of various DERs and energy storage systems in dc microgrids. These research works

aim to overcome the challenge of achieving a decentralized control operation using only local variables. Be that as it may, the DERs in dc microgrids are powerfully joined to each other and there must be a smallest level of organization between the DERs and the controllers. In a half breed air conditioning/dc matrix design that comprises of both ac and dc systems associated together by a bidirectional converter is proposed. Progressive control calculations are incorporated to guarantee smooth power exchange between the air conditioner microgrid and the dc microgrid under different working conditions. However, failure of the bidirectional converter will bring about the isolation of the dc microgrid from the air conditioner microgrid.

2. WIND ENERGY CONVERSION SYSTEMS

2.1 Wind Turbine Technology

The wind turbine is the first and foremost element of wind power systems. There are two main types of wind turbines, the horizontal-axis and vertical-axis turbines.

2.1.1 Horizontal-axis Turbines

Horizontal-axis Turbines (see Figure 2.1) are primarily composed of a tower and a nacelle mounted on top of tower. The generator and gearbox are normally located in the nacelle. It has a high wind energy conversion efficiency, self-starting capability, and access to stronger winds due to its elevation from the tower. Its disadvantages, on the other hand, include high installation cost, the need of a strong tower to support the nacelle and rotor blade, and longer cables to connect the top of the tower to the ground.

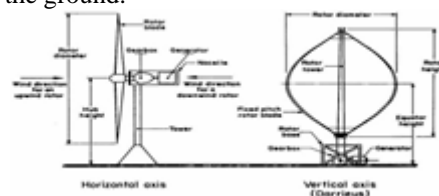


Figure 2.1: illustration of a horizontal axis and a vertical axis wind turbine.

2.1.2 Vertical-axis Turbines

A Vertical axis Turbines' spin axis is perpendicular to the ground (See Figure 3.1). The Wind Turbine is vertically mounted, and its generator and gearbox is situated at its base. Contrasted with even hub turbines, it has decreased establishment cost, and upkeep is less demanding, in light of the ground level apparatus box and generator establishment. Another preferred standpoint of the vertical pivot turbine is that its operation is autonomous of wind course.

2.2 Types of Horizontal-Axis Wind Turbines

2.2.1 Pitched Controlled Wind Turbines

Pitch Controlled Wind Turbines change the introduction of the rotor sharp edges along its longitudinal hub to control the yield control. These turbines have controllers to check the yield control a few times each second, and when the yield control achieves a most extreme edge, a request is sent to the cutting edge water driven pitch component of the turbine to pitch (or to turn) the rotor somewhat out of twist to back off the turbine.

2.2.2 Stalled Controlled Wind Turbines

The rotor blades of a Stall Controlled Wind Turbine are bolted onto the hub at a fixed angle. The blades are aerodynamically designed to slow down the blades when winds are too strong. The stall phenomenon caused by turbulence on rotor blade prevents the lifting force to act on the rotor. The rotor blades are twisted slightly along the longitudinal axis so that the rotor blade stalls gradually rather than suddenly when the wind reaches the turbines' critical value.

2.2.3 Active Stall Controlled Wind Turbines

Active Stall Turbines are very similar to the pitch controlled turbine because they operate the same way at low wind speeds. However, once the machine has reached its rated power, active stall turbines will turn its blades in the opposite direction from what a pitch controlled machine would. By doing this, the blades induces stall on its rotor blades and consequently waste the excess energy in the wind to prevent the generator from being overloaded. This mechanism is usually either realized by hydraulic systems or electric stepper motors.

2.3 Types of Wind Energy Conversion Systems (WECS)

There are two main types of Wind Energy Conversion Systems (WECSs), the fixed speed WECS and variable-speed WECS. The rotor speed of a fixed-speed WECS, also known as the Danish concept, is fixed to a particular speed. The other type is the variable-speed WECS where the rotor is allowed to rotate freely. The variable-speed WECS uses power maximization techniques and algorithms to extract as much power as possible from the wind.

2.3.1 Fixed Speed Wind Energy Conversion Systems

As the name recommends, Fixed Speed Wind Energy Systems work at a consistent speed. The settled speed WECS setup is otherwise called the "Danish idea" as

it is generally utilized and created in Denmark. Ordinarily, enlistment (or non-concurrent) generators are utilized as a part of settled speed WECSs in light of its innate cold-heartedness to changes in torque. The rotational speed of an enlistment machine changes with the compel connected to it, yet practically speaking, the contrast between its speed at top power and out of gear mode (at synchronous speed) is little.

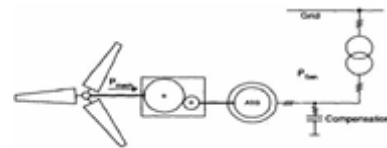


Figure 2.2 A Typical Fixed Speed Wind Turbine Configuration.

2.3.2 Variable Speed Wind Turbine Systems

In Variable Speed Wind Turbine systems, the turbine is not directly connected to the utility grid. Instead, a power electronic interface is placed between the generator and the grid to provide decoupling and control of the system. Thus, the turbine is allowed to rotate at any speed over a wide range of wind speeds.

2.4 Configurations of Variable Speed Wind Conversion Systems

2.4.1 Synchronous Generators

The stator of the Synchronous Generators holds the set of three-phase windings that supply the external load. The rotor, on the other hand, is the source of the machine's magnetic field. The magnetic field is either supplied by a Direct Current (DC) flowing in a wound field or a permanent magnet. Figure 3.3 illustrates a typical setup of a wind turbine with a Wound Field Synchronous Generator (WFSG) connected to the grid through power electronic converters. The WFSG has high machine efficiency, and the power electronic converters allow direct control over the power factor. However, because of the winding circuit in the rotor, the size of the WFSG can be rather large. Another drawback of the configuration in Figure 2.3 is that in order to regulate the active and reactive power, the power electronic converter must be sized typically 1.2 times the rated power. Thus, the use of the WFSG leads to a bulky system.

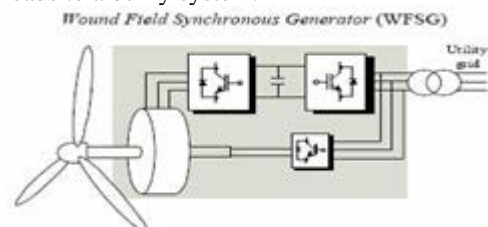


Figure 2.3: A Typical Fixed Speed Wind Turbine Configuration.

3. SYSTEM DESCRIPTION AND MODELING

3.1 System Description

The overall configuration of the proposed dc grid based wind power generation system for the poultry farm is shown in Fig. 3.1. The system can operate either connected to or islanded from the distribution grid and consists of four 10 kW Permanent Magnet Synchronous Generators (PMSGs) which are driven by the variable speed Wind

Turbines(WTs). Instead of using individual inverter at the output of each Wind Generator (WG), the use of two inverters between the dc grid and the ac grid is proposed. During normal operation, the two inverters will share the maximum output from the PMSGs (i.e., each inverter shares 20 kW). The maximum power generated by each WT is estimated from the optimal wind power $P_{wt,opt}$ as follows

$$P_{wt,opt} = k_{opt} (\omega_{r,opt})^3$$

$$k_{opt} = \frac{1}{2} C_p \rho A \left(\frac{R}{\lambda_{opt}} \right)^2$$

$$\omega_{r,opt} = \frac{\lambda_{opt} v}{R}$$

When one inverter fails to operate or is under maintenance, the other inverter can handle the maximum power output of 40 kW from the PMSGs. Thus the proposed topology offers increased reliability and ensures continuous operation of the wind power generation system when either inverter 1 or inverter 2 is disconnected from operation. An 80 Ah Storage Battery (SB), which is sized is connected to the dc grid through a 40 kW bidirectional dc/dc buck-boost converter to facilitate the charging and discharging operations when the microgrid operates connected to or islanded from the grid.

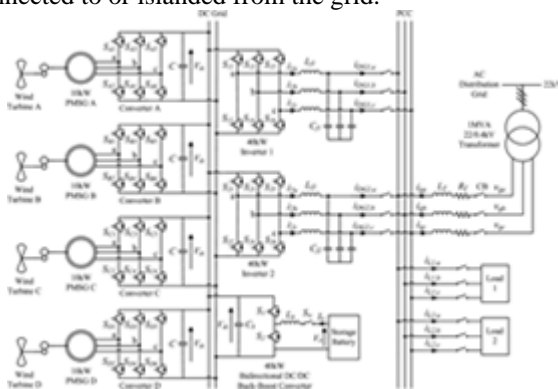


Fig. 3.1. Overall Configuration of the Proposed DC Grid based Wind Power Generation System in a Microgrid.

The energy constraints of the SB in the proposed dc grid are determined based on the System-On-a-Chip(SOC) limits given by

$$SOC_{min} < SOC \leq SOC_{max}$$

Although the SOC of the SB cannot be directly measured, it can be determined through the estimation methods as detailed. With the use of a dc grid, the impact of fluctuations between power generation and demand can be reduced as the SB can swiftly come online to regulate the voltage at the dc grid. During off-peak periods when the electricity demand is low, the SB is charged up by the excess power generated by the WTs. Conversely, during peak periods when the electricity demand is high, the SB will supplement the generation of the WTs to the loads.

3.2 System Operation

When the microgrid is operating connected to the distribution grid, the WTs in the microgrid are responsible for providing local power support to the loads, thus reducing the burden of power delivered from the grid. The SB can be controlled to achieve different demand side management functions such as peak shaving and valley filling depending on the time-of-use of electricity and SOC

of the SB. During islanded operation where the Circuit Breakers (CBs) disconnect the microgrid from the distribution grid, the WTs and the SB are only available sources to supply the load demand.

3.3 AC/DC Converter Modeling

Fig. 4.2 shows the power circuit consisting of a PMSG which is connected to an ac/dc voltage source converter. The PMSG is modeled as a balanced three-phase ac voltage source e_{sa}, e_{sb}, e_{sc} with series resistance R_s and inductance L_s .

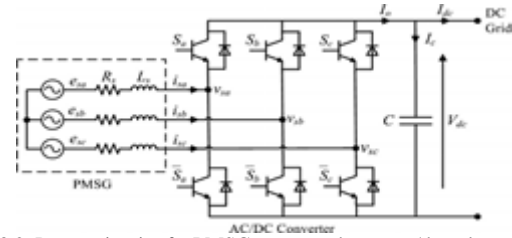


Fig. 3.2. Power circuit of a PMSG connected to an ac/dc voltage source converter.

3.4 DC/AC Inverter Modeling

The two 40 kW three-phase dc/ac inverters which connect the dc grid to the Point of Common Coupling (PCC) are identical, and the single-phase representation of the three-phase dc/ac inverter is shown in Fig. 4.3.

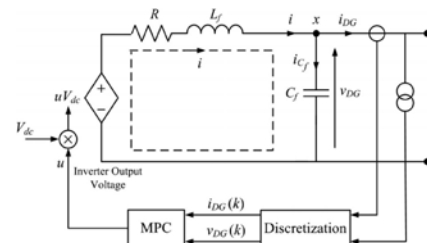


Fig. 3.3. Single-phase representation of the three-phase dc/ac inverter.

During grid-connected operation, the inverters are connected to the distribution grid and are operated in the current Control Mode (CCM) because the magnitude and the frequency of the output voltage are tied to the grid voltage. In this project, the grid is set as a large power system, which means that the grid voltage is a stable three-phase sinusoidal voltage. Hence, when operating in the CCM, a three-phase sinusoidal signal can be used directly as the exogenous input. During islanded operation, the inverters will be operated in the Voltage control Mode (VCM). The voltage of the PCC will be maintained by the inverters when the micro grid is islanded from the grid.

3.5 Control Design for the AC/DC Converter

Fig. 4.4 shows the configuration of the proposed controller for each ac/dc voltage source converter which is employed to maintain the dc output voltage V_{dc} of each converter and compensate for any variation in V_{dc} due to any power imbalance in the dc grid. The power imbalance will induce a voltage error at the dc grid, which is then fed into a proportional integral controller to generate a current reference i^*d for i_d to track. To eliminate the presence of high frequency switching ripples at the dc grid, V_{dc} is first passed through a first-order LPF. The current i_q is

controlled to be zero so that the PMSG only delivers real power. The current errors Δi_d and Δi_q are then converted into the abc frame and fed into a Proportional Resonant(PR) controller to generate the required control signals using pulse-width modulation.

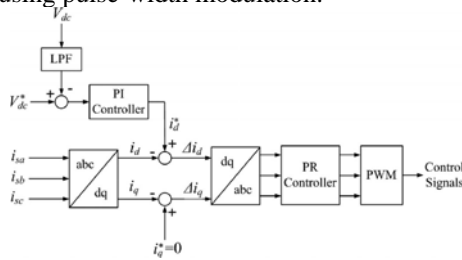


Fig. 3.4. Configuration of the Proposed controller for the ac/dc converter.

3.6 Control Design for the DC/AC Inverter

In order for the microgrid to operate in both grid-connected and islanded modes of operation, a model-based controller using Model Predictive Control(MPC) is proposed for the control of the inverters. MPC is a model-based controller and adopts a receding horizon approach in which the optimization algorithm will compute a sequence of control actions to minimize the selected objectives for the whole control horizon, but only execute the first control action for the inverter. At the next time step, the optimization process is repeated based on new measurements over a shifted prediction horizon. By doing so, MPC can make the output track the reference at the next step, as well as plan and correct its control signals along the control process. This will guarantee a better transient response compared to conventional PID/PR controllers.

4. SIMULATION RESULTS

The simulation model of the proposed dc grid based wind power generation system shown in Fig. 4.1 is implemented in MATLAB/Simulink. The effectiveness of the proposed design concept is evaluated under different operating conditions when the microgrid is operating in the grid-connected or islanded mode of operation.

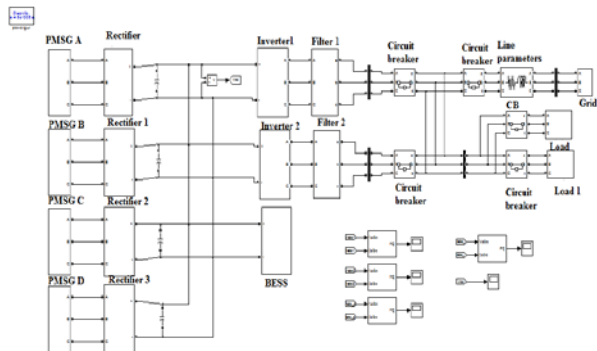


Fig:3.1- simulation diagram of a Failure of One Inverter During Grid-Connected Operation

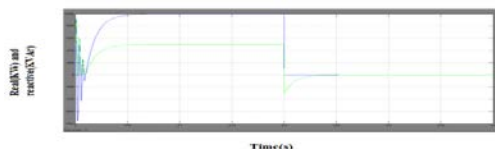


Fig.4.2 Real(top) and Reactive(bottom)Power delivered by inverter1

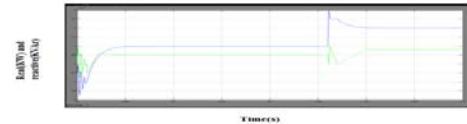


Fig:4.3Real (top) and reactive (bottom) power delivered by inverter 2.



Fig:4.4- Real (top) and reactive (bottom) power delivered by the grid.



Fig:4.5- Real (top) and reactive (bottom) power consumed by the loads.

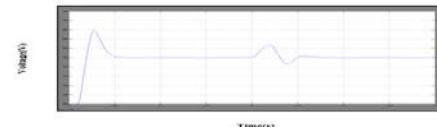


Fig:4.6- DC grid voltage.

Figs. 4.2 and 4.3 show the waveforms of the real and reactive power delivered by inverters 1 and 2 for $0 \leq t < 0.4$ s respectively. For $0 \leq t < 0.2$ s, both inverters 1 and 2 are in operation and each inverter delivers about 10kW of real power and 5kVAr of reactive power to the loads. The remaining real and reactive power that is demanded by the loads is supplied by the grid which is shown in Fig. 4.4. It can be seen from Fig. 4.4 that the grid delivers 40 kW of real power and 5kVAr of reactive power to the loads for $0 \leq t < 0.2$ s. The total real and reactive power supplied to the loads is about 60kW and 12 kVAr as shown in the power waveforms of Fig. 4.5. The unsteady measurements observed in the power waveforms for $0 \leq t < 0.08$ s are because the controller requires a period of about four cycles to track the power references during the initialization period. As shown in Fig. 4.2, the real and reactive power supplied by inverter 1 is decreased to zero in about half a cycle after inverter 1 is disconnected. This undelivered power causes a sudden power surge in the dc grid which corresponds to a voltage rise at $t = 0.2$ s as shown in Fig. 4.6. To ensure that the load demand is met, the grid automatically increases its real and reactive power generation to 50 kW and 10kVAr respectively at $t = 0.2$ sec. *Basic Simulation Diagram of a Connection of AC/DC Converter During Grid- Connected Operation*

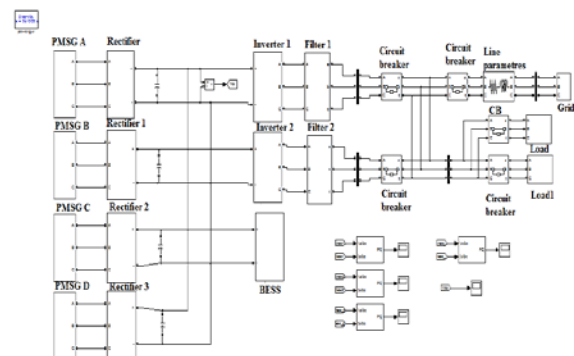


Fig:4.7- simulation diagram of a Connection of AC/DC Converter During Grid-Connected Operation

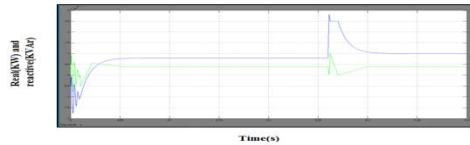


Fig:4.8- Real (top) and reactive (bottom) power delivered by inverter 1.



Fig:4.9- Real (top) and reactive (bottom) power delivered by inverter 2

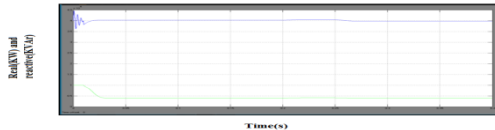


Fig:4.10- Real (top) and reactive (bottom) power delivered by the grid.

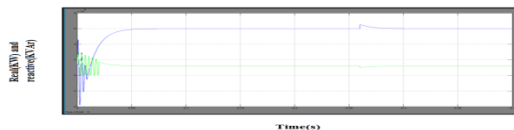


Fig:4.11- Real (top) and reactive (bottom) power consumed by the loads.

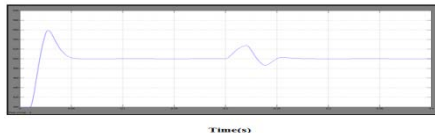


Fig:4.12- DC grid voltage.

The EMS increases the real delivered by each inverter to 10 kW while the reactive power supplied by each inverter remains unchanged at 4 kVAr as shown in Figs. 4.8 and 4.9. This causes a momentarily dip in the dc grid voltage at $t = 0.26$ s as observed in Fig. 4.12 which is then restored back to its nominal voltage of 500 V for $0.26 \leq t < 0.4$ s. The grid also simultaneously decreases its supply to 40 kW of real power for $0.26 \leq t < 0.4$ s while its reactive power remains constant at 4 kVAr as shown in Fig. 4.10. Basic Simulation diagram of a Islanded Operation

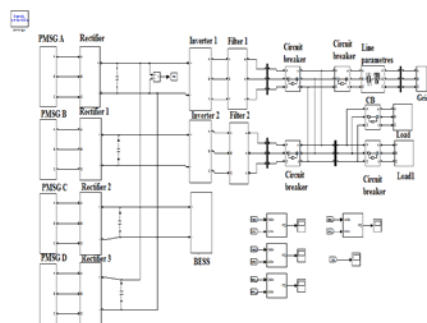


Fig:4.13- simulation diagram of a islanded operation

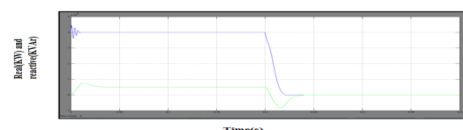


Fig:4.14- Real (top) and reactive (bottom) power delivered by the grid.



Fig:4.15- Real (top) and reactive (bottom) power delivered by inverter 1.

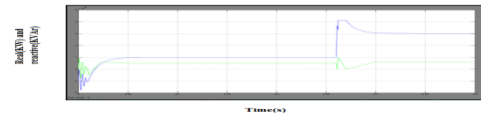


Fig:4.16- Real (top) and reactive (bottom) power delivered by inverter 2.

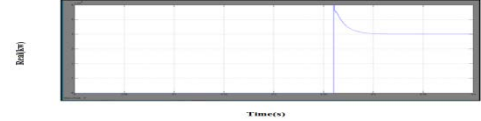


Fig:4.17- Real power delivered by SB.

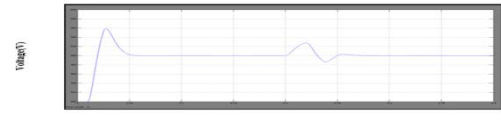


Fig:4.18-DC Grid Voltage

The grid is supplying real power of 40 kW and reactive power of 4 kVAr to the loads for $0 \leq t < 0.2$ s as shown in Fig. 4.14 while each inverter is delivering real power of 10 kW and reactive power of 4 kVAr to the loads as shown in Figs.4.15 and 4.16. At $t = 0.2$ s, the microgrid is disconnected from the distribution grid by the CBs due to a fault occurring in the upstream network of the distribution grid. To maintain the stability of the microgrid, the SB is tasked by the EMS to supply real power of 40 kW at $t = 0.26$ s as shown in Fig. 4.17. At the same time, the real and reactive power delivered by each inverter is also increased by the EMS to 30 kW and 6 kVAr as shown in Figs. 4.15 and 4.16 respectively. Fig. 4.18 shows the dc grid voltage where slight voltage fluctuations are observed at $t = 0.26$ s. The initial voltage rise at $t = 0.26$ s is due to the power supplied by the SB while the subsequent voltage dip is due to the increase in power drawn by the inverter

5. CONCLUSION

In this paper, the design of a dc grid based wind power generation system in a microgrid that enables parallel operation of several WGs in a poultry farm has been presented. As compared to conventional wind power generation systems, the proposed microgrid architecture eliminates the need for voltage and frequency synchronization, thus allowing the WGs to be switched on or off with minimal disturbances to the microgrid operation. The design concept has been verified through various test scenarios to demonstrate the operational capability of the proposed microgrid and the simulation results has shown that the proposed design concept is able to offer increased flexibility and reliability to the operation of the microgrid. However, the proposed control design still requires further experimental validation because measurement errors due to inaccuracies of the voltage and current sensors, and modeling errors due to variations in actual system parameters such as distribution line and transformer impedances will affect the performance of the controller in practical implementation. In addition, MPC relies on the accuracy of model establishment; hence further research on improving the controller robustness to modeling inaccuracy is required. The simulation results obtained and the analysis performed in this project serve as a basis for the design of a dc grid based wind power generation system in a microgrid.

REFERENCES

- [1] M. Czarick and J. Worley, "Wind turbines and tunnel fans," *Poultry Housing Tips*, vol. 22, no. 7, pp. 1–2, Jun. 2010.
- [2] The poultry guide: Environmentally control poultry farm ventilation systems for broiler, layer, breeders and top suppliers. [Online]. Available: <http://thepoultryguide.com/poultry-ventilation/>
- [3] Livestock and climate change. [Online]. Available: <http://www.worldwatch.org/files/pdf/Livestock%20and%20Climate%20Change.pdf>.
- [4] Farm Energy: Energy efficient fans for poultry production. [Online]. Available: <http://farmenergy.exnet.iastate.edu>.
- [5] A. Mogstad, M. Molinas, P. Olsen, and R. Nilsen, "A power conversion system for offshore wind parks," in *Proc. 34th IEEE Ind. Electron.*, 2008, pp. 2106–2112.
- [6] A. Mogstad and M. Molinas, "Power collection and integration on the electric grid from offshore wind parks," in *Proc. Nordic Workshop Power Ind. Electron.*, 2008, pp. 1–8.
- [7] D. Jovic, "Offshore wind farm with a series multi terminal CSI HVDC," *Elect. Power Syst. Res.*, vol. 78, no. 4, pp. 747–755, Apr. 2008.
- [8] X. Lu, J. M. Guerrero, K. Sun, and J. C. Vasquez, "An improved droop control method for DC micro grids based on low bandwidth communication with DC bus voltage restoration and enhanced current sharing accuracy," *IEEE Trans. Power Electron.*, vol. 29, no. 4, pp. 1800–1812, Apr. 2014.
- [9] T. Dragicevi, J. M. Guerrero, and J. C. Vasquez, "A distributed control strategy for coordination of an autonomous LVDC microgrid based on power-line signaling," *IEEE Trans. Ind. Electron.*, vol. 61, no. 7, pp. 3313–3326, Jul. 2014.
- [10] N. L. Diaz, T. Dragicevi, J. C. Vasquez, and J. M. Guerrero, "Intelligent distributed generation and storage units for DC micro grids—A new concept on cooperative control without communications beyond droop control," *IEEE Trans. Smart Grid*, vol. 5, no. 5, pp. 2476–2485, Sep. 2014.